Theoretical and Experimental study of the corrosion inhibition of mild steel in acid medium using some surfactants of the essential oil of FoeniculumVulgare bulb

A. Bouoidina[1,2], F. El-Hajjaji[2], A. Abdellaoui[3], Z. Rais[2], M. Filali Baba[2], M. Chaouch[1], O. Karzazi[2], A. Lahkimi[2], M. Taleb[2]

[1]Laboratoire de génie des Matériaux et environnement, Faculté des Sciences, Université Sidi Mohammed Ben Abdellah, Fès, Morocco.

[2]Laboratoire d'Ingénierie d'Electrochimie de Modélisation et Environnement Faculté des Sciences, Université Sidi Mohammed Ben Abdellah, Fès, Morocco.

[3]Laboratoire de Physiologie, Pharmacologie et Santé Environnementale, Faculté des Sciences, Université Sidi Mohammed Ben Abdellah, Fès, Morocco.

Abstract

Corrosion inhibition by Foeniculum vulgare bulb (FVB) essential oil on mild steel was studied in 1 M HCl solution by using the electrochemical techniques and the weight loss measurements. The results obtained clearly revealed that FVB extract behaves as a mixed-type inhibitor and adsorbed physically onto the mild steel surface. The inhibition efficiency increased with increasing concentration of FVB and finally reached 89.2% at 303 K, This behavior decreased with increase in temperature. The most noteworthy inhibition efficiency was affirmed by identification of the film formed on the metal surface by using the scanning electron microscopy (SEM) and energy dispersion X-ray spectroscopy (EDX). The analysis of the chemical composition of the oil allows determining the major constituents all of which are in the form of oxygenated monoterpenes whose trans anethole is the major compound, these molecules are fully optimized by using gradient corrected DFT at B3LYP/6-31G level with Gaussian 09 program, in order to determine the structural and electronic parameters of the molecule responsible for imparting on the extract its high inhibition efficiency.

1. Introduction

The employments of acids, salt and alkaline solutions in industrial applications cause extensive severe corrosion of metal, which prompts tremendous financial misfortunes. These issues had welcomed the consideration of scientific researchers to look for control the corrosion and they found that the utilization of inhibitors is a recognizable strategy to control this phenomenon.

The inhibitors become very used in the protection of materials in several environments [1-2], they can adsorb on the steel surface, block the active sites and decreasing the corrosion rate [3]. Currently, researchers have been working on green inhibitors (environmental friendly) to stay away from the harmful impact of prepared inhibitors. These inhibitors are found to be extremely active in corrosive solutions. Furthermore,they are financial valuable and eco-friendly. The adsorption of inhibitors on the metal surface depends mainly on the physicochemical properties of the inhibitor group, such as the functional group, electron density at donor site [4-12]. Many research works have been developed in order to study the inhibition efficiency of organic molecules according to the physicochemical properties [13–16] and the quantum chemical calculations have been widely used to study reaction mechanisms and to interpret the experimental results as well as to resolve chemical ambiguities [17].

The aim of the present work is to study of mild steel in acid medium, the inhibition efficiency of essential oil extracted from the bulb of foeniculum vulgar. The behavior of this compound in 1.0 M HCl has been studied and its protection efficiency has been determined by Weight loss measurements, polarization and EIS measurements. The steel surface was also examined by scanning electron microscopy (SEM). And then, quantum chemical calculations by DFT method were performed to elucidate the interaction between the main constituents of the crude extract and mild steel surface.

Figure1. Bulb of the FoeniculumVulgare plant

2. Experimental details

The investigated steel materials of chemical composition in weight (0.2% C, 0.38% Si, 0.09% P, 0.01% Al, 0.05% Mn, 0.05% S) are used for the weight loss technique. The samples of mild steel were mechanically polished with different emery paper SiC (grade 120, 1200) before each experiment, washed with distilled water and acetone and finally dried at room temperature. The aggressive solution 1 M HCl is prepared by dilution of Analytical Grade 37% HCl with bidistilled water and the concentration range of inhibitors was 0.4–1 g/l. Gravimetric measurements were carried out in a double walled glass cell equipped with a thermostat-cooling condenser, before immersion. The initial weight of each specimen was noted using an analytical balance, then the specimens were immersed in HCl solutions with and without inhibitors. After 6 h of immersion at 308Kand 2 h for the different temperature (318-348 K), the specimens were washed and reweighed.

Electrochemical measurements were conducted using a potentiostat PGZ100 piloted by VOLTAMASTER software and connected to a conventional three electrode cylindrical Pyrex glass cell. The working electrode (WE) had the form of a disc cut from the steel sheet, a saturated calomel electrode (SCE) was used as reference and a platinum plate was used as counter electrode. Before all experiments, the potential was stabilized at free potential during 30 min, the polarization measurements were performed by applying a controlled potential scan automatically from –800 to –200 mV at a scan rate of 1 mV/s [18].

 A 10 mV peak to- peak sine wave over an frequency range extending from 10 mHz to 100 MHz was used for the impedance measurements. All tests have been performed in non-deaerated solutions and the impedance diagrams are given in the NYQUIST representation. All electrochemical studies were made at 308 K for an immersion time of 1 h, with different concentrations of inhibitor.

For theoretical study of complete geometry of molecules optimized at the DFT B3LYP level, we used 6-31G basis set with Gaussian 9 program. In general, density functional theory method (DFT) is widely used to provide accurate geometries and electronic properties for a wide range of organic compounds [19- 22].

3. Results and discussion

3.1. Components identification

The bulb of foeniculum vulgar (Fennel) was collected in February 2016 in the region of Fes (Morocco). The extraction was carefully performed in the laboratory of Physiology, Pharmacology and Environmental Health in Fez by hydrodistillation using a Clevenger-type apparatus. The various chemical components were analyzed and identified by gas chromatography (GC Ultra Trace), coupled with a type of mass spectrometer (Polaris Q). Data was gathered in table 1. Fig 2 shows the peaks which were identified by comparing retention times with those listed in a type library (NIST-MS). The major components are: Trans anethole (94 %), estragole (2.1 %), Limonène (3.03 %). they are all oxygenated monoterpenes representative for 99.13 % of the total weight with a large dominance of Trans anéthole, its molecular structure is shown in Figure 3.

3.2. Tafel polarization

Fig.4 shows the polarization curves in 1 M HCl with different concentrations of FVB at 30 C. The various electrochemical parameters were calculated from the plots and shown in Table 2. The inhibition efficiency for each concentration of inhibitors is calculated using Eq. (1), where, I_{corr} and I_{inh} are corrosion current densities without and with different concentrations of inhibitors.

$$IE\ \% = \left(\frac{\text{Icorr} - \text{Iinh}}{\text{Icor}}\right) \times 100 \qquad (1)$$

As it can be seen, as the concentration of FVB increased, the value of I decreased and hence the inhibition efficiency increased, reaching a maximum value at 89.2% at 1g/l FVB, on the other hand, there is a small shift in the corrosion potential, which indicated that FVB exhibits both cathodic and anodic inhibition effects. This suggested a mixed-type control and FVB mainly acts as a mixed-type inhibitor in 1 M HCl.
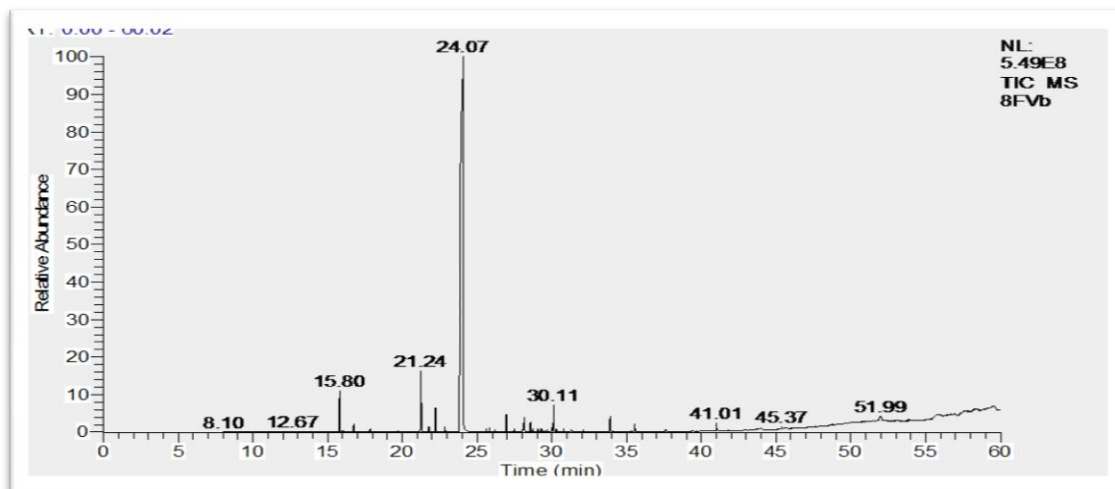
Figure 2. Chromatographic profile of FVB

Table 1. Chemical composition of FVB

Chemical compounds	TR (min)	Formulae	Surface (%)
Estragole	15,87	C10H12O	2,1
Limonène	21,27	C10H16	3,03
Transanethole	24,16	C10H12O	94
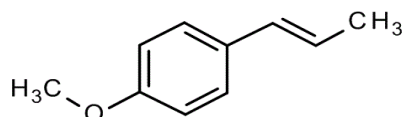
Figure 3. Chemical structure of trans-anethole
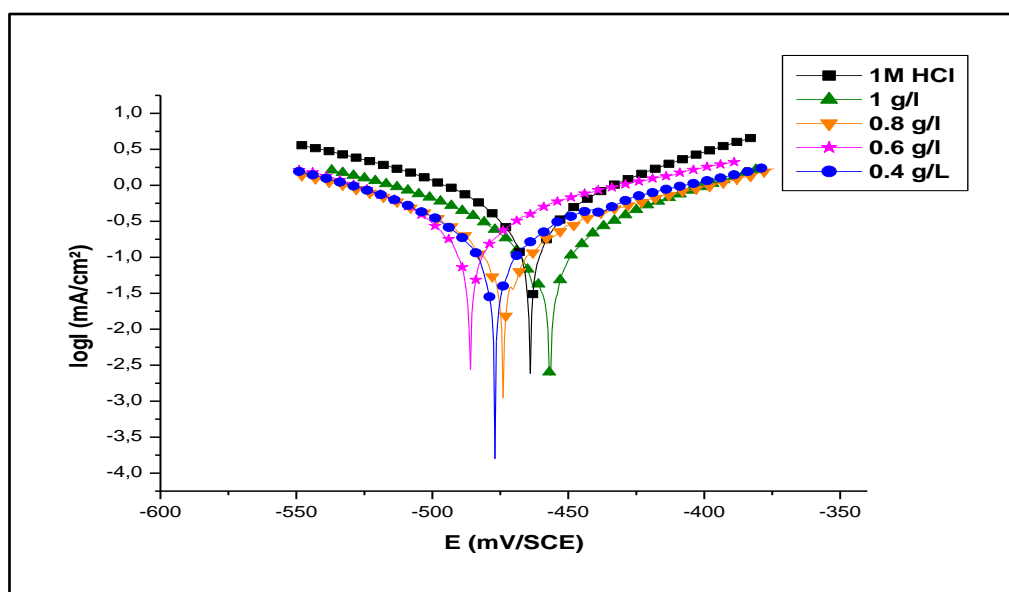
Figure 4. Polarization curves in 1 M HCl solution containing different concentration of FVB

Table 2. Corrosion parameters derived from polarization 1M HCl at different concentrations of inhibitors

inhibitor	C(g/l)	E_{corr}(mV/SCE)	I_{cor}(mA/cm²)	_ßc(mV)	E(%)
Blank	1M HCl	-464	1,879	208,1	
FVL	1	-456,1	0,2036	85,5	89,2
	0,8	-486,1	0,2693	74,2	85,7
	0,6	-472,1	0,2761	108,9	85,3
	0,4	-477	0,2786	96,5	85,2

3.3 Electrochemical impedance spectroscopy (EIS)

The corrosion behaviour of mild steel in the presence of FVB was investigated also by EIS. A typical set of Nyquist plots are shown in Fig.5. Values of associated electrochemical parameters and corrosion inhibition efficiency E% are given in Table 3.
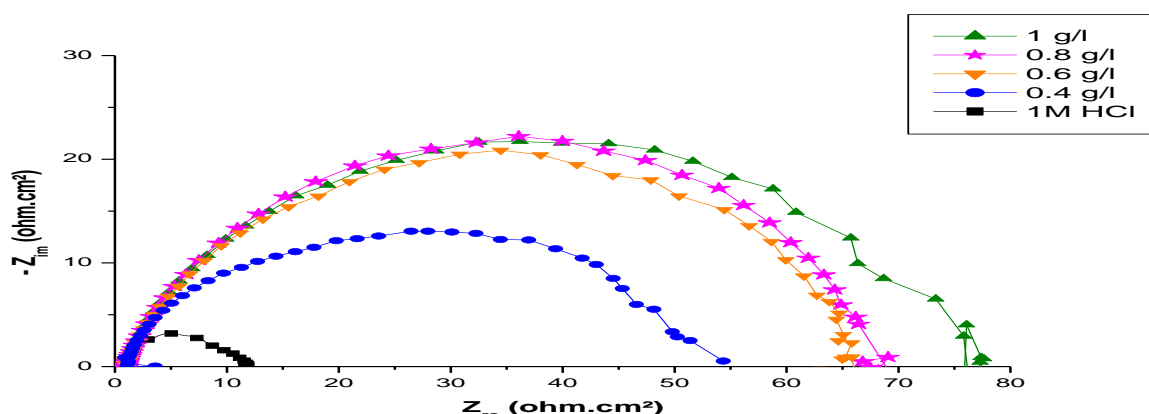
Figure 5. Nyquist diagrams for mild steel in 1 M HCl containing different concentrations of FVB.

Table 3. Impedance parameters and inhibition efficiency for the corrosion of mild steel in 1 M HCl without and with addition of various concentrations of FVB at 308 K

inhibitor	C(g/l)	Rtc (Ω.cm²)	Rs (Ω,cm²)	Cdc (uF/cm⁻²)	E (%)
Blank	1M HCl	11,76	0,820	145,4	
FVB	1	74,2	1,7	23	84,1
	0,8	68,2	1,4	26	82,7
	0,6	66,7	1,3	26	82,4
	0,4	54,5	0,6	32	78,4

It is clear that all impedance spectra exhibit a single depressed semicircle. The single semicircle can be attributed to the charge transfer process that takes place at electrode/solution interface, and the transfer process controls the corrosion reaction of FVB [23], also the Nyquist plots are not perfect semicircles which can be attributed to the frequency dispersion as a result of the roughness and inhomogeneous of the electrode surface [24, 25], the impedance response for mild steel in 1 M HCl solutions changes significantly with increasing inhibitor concentration. The greatest effect was observed at a concentration 1g/l. The results obtained from the E.I.S. correspond to those from the polarisation curves tests. Furthermore, they can be simulated using the equivalent circuit shown in Fig. values were calculated from the difference in impedance at lower and higher frequencies, as suggested in Ref [26],the double layer capacitance is affected by imperfections of the surface, and that this effect is simulated via a constant phase element (CPE) [27,28], this parameter (CPE) quantifies different physical phenomena like surface inhomogeneous resulting from surface roughness, porous layer

formation, inhibitor adsorption, etc. So the capacitance is deduced from the following Eq.2 by determining the frequency at which the imaginary component of the impedance was the maximum:

$$Cdc = \frac{1}{2\pi f - Zmax \; Rp} \qquad (2)$$
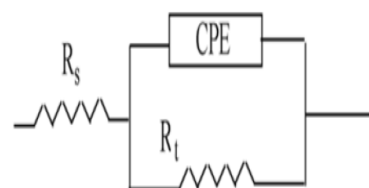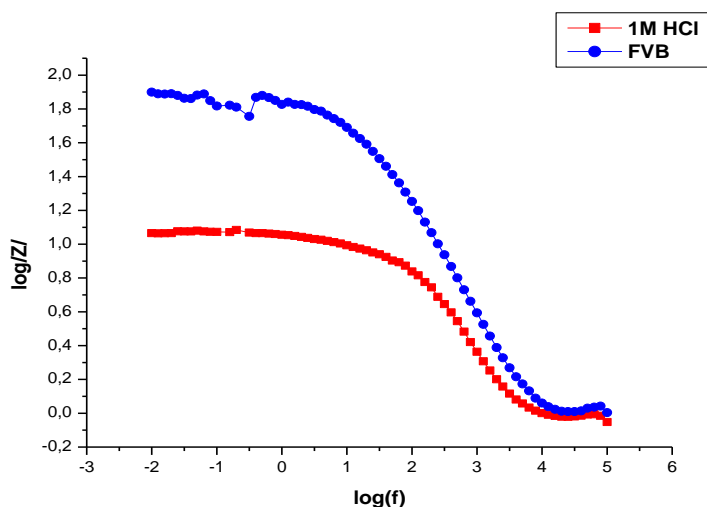
Figure 6. Bode diagrams for steel in 1 M HCl.   **Figure 7.** Equivalent circuit model for impedance analysis

The equivalent circuit constituted of a constant phase element (CPE) to account for heterogeneity previously described, the resistance of the electrolyte (Rs) and charge transfer resistance (Rt) is proposed to represent the steel mild in HCl (Fig.7). An excellent fit of the spectrum of the FVS solution 1 g / l is obtained with the equivalent circuit using Z_{View}. To confirm the choice of circuit it is necessary to analyze another representation of the impedances: the representation of Bode (Fig.6). The impedance diagram recorded in Bode mode for FVB solution 1g/l shows only one time constant, two levels indicating that it is the charge transfer process taking place in the steel / solution interface.

3.4. Weight loss measurements
The corrosion rates of mild steel were determined using Eq.3

$$W = \frac{\Delta m}{st} (3)$$

WhereΔm is mass loss, s is the area of specimen and t is immersiontime. The inhibition efficiencies were calculated using Eq.4, where Wcorr and Winh are the values of the weight loss of steel after immersion in solutions without and with inhibitor, respectively.

$$IE \% = \left(\frac{Wcor - Winh}{Wcor}\right) \times 100 \qquad (4)$$

Table 4. Gravimetric results of steel in acid without and with addition of the FVS (t=6h. T= 298±1 K).

C (g/l)	Wcorr (mg.cm^{-2}.h^{-1})	Ew (%)
HCl 1M	0,6134	
1	0,0578	90,6
0,8	0,0633	89,7
0,6	0,0725	88,2
0,4	0,0779	87,3

Table 4 gives values of corrosion rate of mild steel and percentage inhibition efficiency calculated from the weight loss measurements for different concentrations of FVB. It can be concluded that, the corrosion rate of mild steel decreased when the inhibitor concentration increased, by against the inhibition efficiency increased

with increasing inhibitor concentration. As it is seen, the inhibition efficiencies obtained from weight loss measurements area little lower than the efficiencies obtained from electrochemical experiments, this phenomenon attributed to the fact that weight loss experiments gives average corrosion rates, contrariwise the electrochemical experiments gives instantaneous corrosion rates [29].We can then say that the gravimetric measurements obtained from weight loss and electrochemical measurements are in good agreement.

3.5. *Effect of temperature*
In order to calculate thermodynamic activation parameters of the corrosion processes of steel in acidic media, the effect of temperature was studied in the absence and presence of optimum concentration of inhibitor: 1g/l in the temperature range 318-348K during 2h of immersion. The variation of inhibition efficiency (E%) and the corrosion rate (Wcorr) at different temperatures are listed in Table 5.

Table 5. Influence of temperature on the corrosion rate and inhibition efficiency of mild steel in 1 M HCl at 2g/l (t=2h)

T (K)	1M HCl W_{corr} (mg.cm^{-2}.h^{-1})	inhibitor W_{corr} (mg.cm^{-2}.h^{-1})	E_w (%)
318	1,85	0,28	85,1
328	2,73	0,45	83,6
338	3,99	0,85	78,6
348	5,42	2,69	50,5

The results obtained show an increase in the corrosion rate and decrease in IE% with increasing temperature. The dependence of corrosion rate with temperature can be expressed by the Arrhenius equation (Eq.5, 6), from which The activation parameters for the studied system can be estimated [30, 31], where A is Arrhenius factor, Ea is the apparent activation corrosion energy, h is the Plank's constant, N is the Avogadro's number, and ΔH^*a and ΔS^*a are the enthalpy and the entropy changes of activation corrosion energies for the transition state complex. R is the perfect gas constant.

$$Icorr = A\exp(\frac{-Ea}{RT}) \qquad (5)$$
$$Icorr = \frac{RT}{Nh}\exp\left(\frac{\Delta Sa*}{R}\right)\exp(\frac{-Ha*}{RT}) \qquad (6)$$

Table 6. The values of activation parameters for mild steel in 1M HCl in the absence and the presence of 1 g/L of FVS

Thermodynamiq data	**Ea** (kj/mol)	**ΔH** (kj/mol)	**ΔS** (j.K^{-1} mol^{-1})
1M HCl	33	31	-159
FVB	69.2	66.5	-64.2

The activation parameters for the corrosion process in absence and presence of inhibitors are given in Table 6. From these results, we remark that increase in corrosion activation energy in the presence of inhibitor compared to its absence is interpreted as being suggestive of formation of an adsorption film of physical nature (physisorption) [32,33].
The positive values of ΔH* show that the corrosion process is an endothermic phenomenon and that the dissolution of mild steel is difficult [34]. The negative signof ΔS* shows that the activated complex in the rate determining step represents an association rather than a dissociation step, meaning that a decrease in disordering takes place on going from reactants to the activated complex [35].

3.6. *SEM analysis*
In order to prove the formation of adsorption film on the mild steel surface in the presence of FVB, an analysis of the mild steel surface by the scanning electron microscope was carried before immersion (Fig.8.a) and after immersion in 0.1 M HCl in the absence (Fig.8.b) and presence of 1 g/l of FVB (fig.8.c)
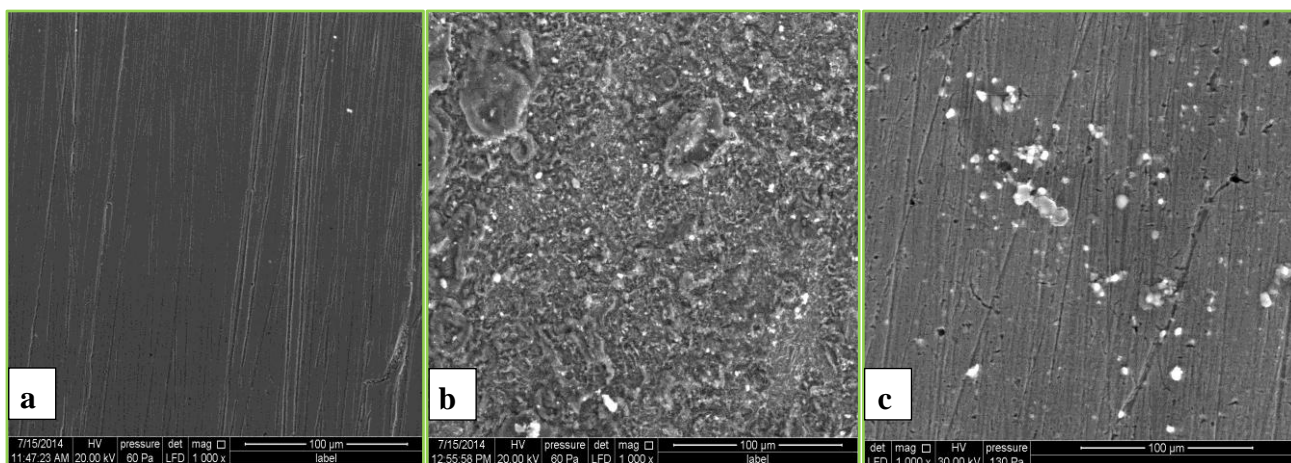
Figure 8. SEM images of mild steel (a) polished, (b) after immersion in acid solution (1 M HCl) without inhibitors, (c) after immersion in acid solution (1 M HCl) containing 1g/l of FVB.

It can be seen that the corrosion surface of mild steel no immersed in the solution is obviously different from the corroded one in the absence or presence of inhibitor, it appeared to be relatively uniform in rough (Fig.8.a).The narrow furrow presented in the uncorroded surface may be attributed to the polished trace by emery papers. as It can be found that the steel surface in 1 M HCl in the absence of FVB looks rather uneven and appears potholed shape while the surface immersed in the aggressive solution containing 1 g/l inhibitor became flat and closely packed in (Fig.8.b), which suggested that an adsorption layer of inhibitors formed on the surface and protected the metal from aggressive corrosion. The above phenomenon suggested that FVB provided better protection in the acid, corresponding to the results of corrosion inhibition obtained from the electrochemical analyses.

3.7. *EDX Analysis*

The EDX analytical technique can be used for the elemental analysis and for the determination of the specimen composition. X-rays that have sufficient energy to escape the material surface can be detected, resulting in a spectrum with peaks of the characteristic energies for the elements present (Fig.9). The areas under selected peaks can also be used to provide semi-quantitative elemental composition information. The results of EDX spectra of mild steel before and after the exposure to the inhibitor solution containing 1g/l of FVB for 6h displayed in the table7.

Indeed, after mild steel has been immersed in the absence and presence of FVB for 6h, we note that the appearance of a new oxygen peak (Fig B, C) compared with the spectrum of mild steel not submerged (Fig A). By comparing the three spectra, the new oxygen peak due to the formation of iron oxides resulting from corrosion of steel in 1 M HCl solution with and without inhibitor.Furthermore, in inhibited solution, the O signal is significantly reduced (Table 7).These data confirms that inhibitor molecule precludes the formation of iron oxide and inhibits the corrosion through its strong adsorption on the mild steel surface.

1.6. *Quantum chemical calculation*

Researchers noted that the adsorption on the metal surface depends mainly on the physicochemical properties of the inhibitor group, such as the functional group, electron density at donor site and π orbital character [36-38].In this context, the Density Functional Theory (DFT) has been recently used to describe the interaction between the inhibitor molecule and the surface as well as the properties of these inhibitors concerning their reactivity [39-40]. This study is carried out by the method B3LYP / 6-311G (d, p).

Frontier orbital theory is useful in predicting the adsorption of molecularcenters responsible for the interaction with surface metal atoms [41].The structures of major constituents of the extractin the isolated statewere first optimized using DFT calculations, and HOMO and LUMO populations of inhibitors are shown in Fig.10

From the molecular orbital density distribution, we can see that the distribution of HOMO is localized on the entire molecule of the three compounds.The LUMO orbitals show the same behaviour as the HOMO orbitals. These active sites ensure strong interaction of molecule with the metal surface. In the same trend, the reactivity of a molecule is governed by the frontier orbitals. It is the energy of the highest occupied molecular orbital (EHOMO), which indicates the ability of a molecule to donate electrons to an acceptor molecule and the energy. On the other hand, the lowest unoccupied molecular orbital (ELUMO) predict the regions where the molecules can accept electrons from the metal using antibonding orbitals to form feedback bonds [42]
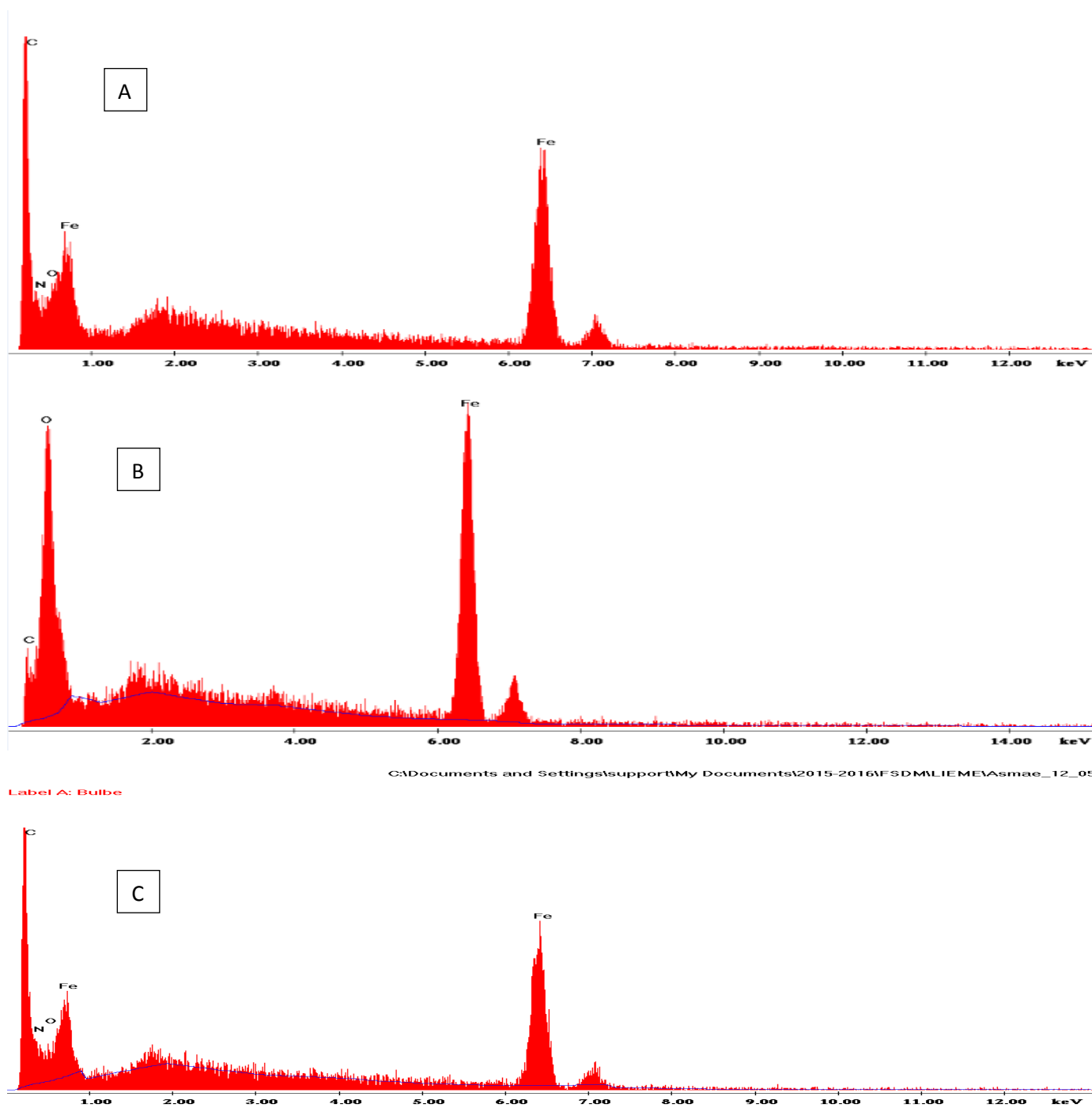
Figure 9. EDX spectrum of mild steel (A) dry, (B) after immersion in 1 M HCl solution without inhibitor (C) after immersion in 1M HCl solution containing 1 g/l of FVB.

Table 7. Percentage in mass obtained from EDX analyzes of the different elements composing the mild steel surface, (A) dry steel, (B) after immersion in 1 M HCl solution without inhibitor (C) after immersion in 1M HCl solution containing 1 g/lof FVB.

Elements		Fe	C	O
W_t	A	83.53	16.47	
	B	67.98	13.81	18.21
	C	31.04	61.95	7.00

A1)
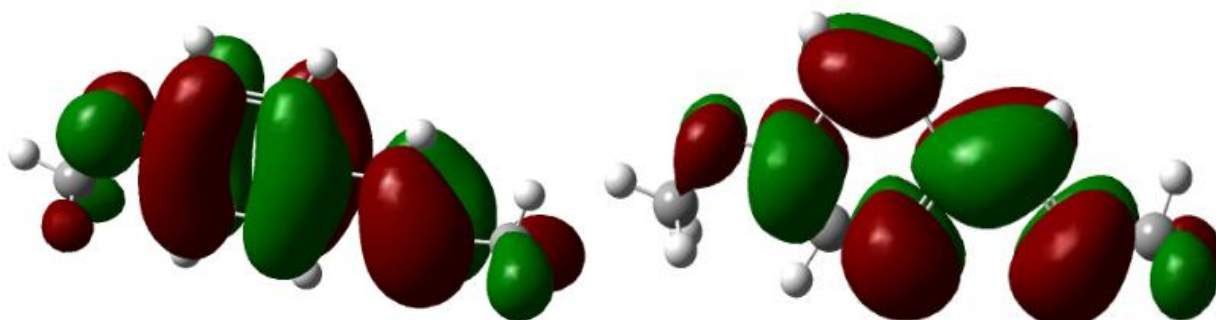
A2)
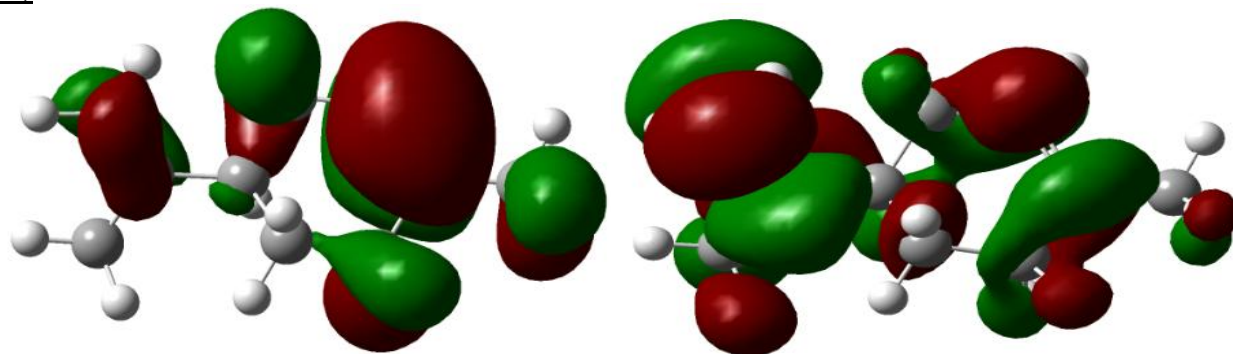
A3)
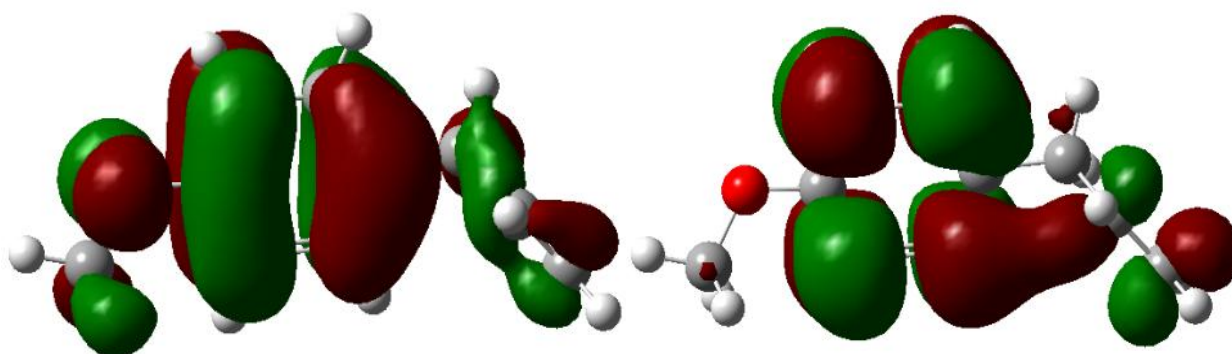
Figure 10. HOMO (center) and LUMO(right) molecular orbitals of A1) Trans-anetholeA2) Limonene A3) Estragolobtained with the DFT at B3LYP/6-31G (d,p) level.

Our approach in this investigation involve the analysis of the electronic parameters of the main constituents of the extract such as the highest occupied molecular orbital energy (EHOMO), the lowest unoccupied molecular orbital (ELUMO), energy gap (ΔE), electronegativity (χ), Dipole moment (μ), electron affinity (A), Ionization potential (I), hardness (η), softness (σ), electron charge transfer (ΔN). These parameters obtained from the optimized structures are estimated using the equations [43-50] :

$$\Delta E_{gap} = E_{LUMO} - E_{HOMo} \qquad (7)$$
$$I = -E_{HOMO} \qquad (8)$$
$$A = -E_{LUMO} \qquad (9)$$
$$\chi = \frac{I+A}{2} \qquad (10)$$
$$\mu = -\chi \qquad (11)$$
$$\eta = \frac{I-A}{2} \qquad (12)$$
$$\sigma = \frac{1}{\eta} \qquad (13)$$
$$\Delta N = \frac{\chi(Fe) - \chi(inh)}{2(\eta(Fe) + \eta(inh))} \qquad (14)$$

In Table 4, we have grouped the values of Quantum chemical parameters of the molecules of Transanethole (A1), limonene (A2) and estragol (A3). The values of χ (Fe) and η (Fe) are taken as 7 eV/mol and 0 eV/mol respectively.

Table8. The quantum descriptors of A1, A2 and A3 calculated using DFT at B3LYB/6-31G (d, p)

parameter	E_{HOMO} (eV)	E_{LUMO} (eV)	ΔE (eV)	A (eV)	I (eV)	X (eV)	μ (D)	η (eV)	σ (eV^{-1})	ΔN
A1	-5.322	-0.453	4.869	0.453	5.322	2.888	1.408	2.435	0.411	0.845
A2	-6.132	0.750	6.883	-0.750	6.132	2.691	0.652	3.441	0.291	0.626
A3	-5.710	0.023	5.734	-0.023	5.710	2.843	1.170	2.867	0.349	0.725

By comparing the three compounds: A1, A2 and A3, the calculations show that the compound A1 has the highest HOMO level (-5.322 eV) and the lowest LUMO level at (-0.453 eV) compared to the obtained parameters for A2 (-6.132 and 0.75 eV) and A3 (-5.710 and 0.023 eV). This can predict a higher inhibitory efficiency of A1, which will be due to the increasing energyof the HOMO and the decreasing energy of the LUMO. It has been documented that the higher the energy level of HOMO, the less is the value of the ionization potential, and the easier for electrons to be easily donated [51]. Organic molecules with less negative HOMO value corresponds to lower I values and is expected to have greater adsorption ability to metal surface.

The difference between the HOMO and the LUMO energies (ΔE) is an important parameter as a function of reactivity of the inhibitor molecule towards the adsorption on metallic surface (physisorption and chemisorption), the inhibitor with a small ΔE should exhibit a higher interaction with the metal surface. The results obtained show that the compound A1 has a lower ΔEgap. This parameter provides a measure for the stability of the inhibitor molecule towards the adsorption on the metal surface. As ΔEgap decreases, the reactivity of the molecule increases leading to increase the inhibition efficiency of the molecule. The value of ΔEgap for A1, A2 and A3 are +4.869, +6.883 and +5.734 eV, respectively. The results as indicated in Table 8 shows that inhibitor A1 has the lowest energy gap than A2 and A3, this means that the molecule could have better performance as corrosion inhibitor.

Dipole moment μ (Debye) is another important electronic parameter that results from non-uniformed distribution of charges on the various atoms in the molecule. The inhibitor with high dipole moment tend to form strong dipole–dipole interactions with the metal surface, resulting in strong adsorption on the surface of the metal and therefore leading to greater inhibition efficiency [52-53]. The energy of the deformability increases with the increase in Dipole moment, making the molecule easier to adsorb. The volume of the inhibitor molecules also increases with the increase of μ. This increases the contact area between the molecule and surface of metal and increasing the corrosion inhibition ability of inhibitors. In our case, the value +1.408(Debye) of A1 enumerates its better inhibition efficiency than A2 and A3 and suggests that it is very reactive compound.

Softness (σ)and Absolute hardness (η) are important properties to measure the molecular stability and reactivity. First of all, it is apparent that the chemical hardness fundamentally signifies the resistance towards the deformation / polarization of the electron cloud of the atoms, ions or molecules under small perturbation of chemical reaction. According to the hard–soft acid base (HSAB) principle, a hard molecule is associated with low basicity signifies a low electron donating ability and a soft molecule is associated with greatbasicity and high electron donating tendency [54-55] Suggesting that the inhibition efficiency increases with increasing softness and decreases on increasing the hardness of the molecules. In our present study A1 has a low hardness value (2.435 eV) and a high value of softness (0.411) compared with other compound A2 (3.441 / 0.291 eV) and A3 (2.867 / 0.349 eV), respectively.

For the amount of charge transfer ΔN between the molecules and the mild steel surface. A positive value of ΔN indicates that the molecules act as an electron acceptor, while a negative value indicates that the molecules act as electron donors [56]. From Table 2, all the molecules studied act as electron acceptors. According to Lukovits, if ΔN < 3.6, the molecules can be assumed to possess charge transfer ability towards the metal surface [57]. The information got from the present study demonstrated that the molecules studied possess charge transfer abilities towards mild steel.

Conclusion

The results of our work revealed that the essential oil of the Foeniculum vulgare bulb worked as a very-good green inhibitor having great inhibitive properties for mild steel in 1 M HCl. The inhibition efficiency has maximum value equal to 89.2% at the highest concentration of oil and diminishes with a rise in temperature.

The main constituents of extract of Foeniculum vulgare bulb are transanethole, limonene and estragol, they are all in the form of oxygenated monoterpenes whose trans anethole is the major compound (94%). The high performance of the extract may be due to the synergistic effect of these compounds especially that the molecules differ considerably in their chemical structures and we do not yet know their individual inhibition efficiencies.

The anticorrosion investigation of the extract by the various methods: Tafel polarization curves, electrochemical impedance spectroscopy and the weight loss measurements clearly revealed its role in the protection of metal surface in corrosive solution. This is justified by the formation of a protective-film on the mild steel surface when analyzedby Scanning electron microscopy and dispersion X-ray spectroscopy

More than this, the density functional theory (DFT) has successfully been used to gain some insights into chemical reactivity and mechanism of corrosion inhibition of extract at the molecular level.

References

1. El Malki Z., Bouachrine M., Hamidi M., Bejjit L., Haddad M., *J. Mater. Environ. Sci.* 1 (S1) (2010) 337.
2. Ghazoui A., Benchat N., El-Hajjaji F., Taleb M., Rais Z., Saddik R., Elaatiaoui A., Hammouti B., *Journal of Alloys and Compounds* 693 (2017) 510.
3. Al Mamari K., Elmsellem H., Sebbar K., Elyoussfi A., Steli H., Ellouz M., Ouzidan Y., Nadeem A., Essassi E.M., El-Hajjaji F., *J. Mater. Environ. Sci.* 7 (9) (2016) 3286.
4. Singh A.K., Quraishi M.A., Corros. Sci. 52 (2010)152.
5. Zarrouk A., Hammouti B., Dafali A., Bentiss F., *Ind. Eng. Chem. Res.*52 (2013) 2560.
6. De Sauza F.S., Spinelli A., *Corros. Sci.* 51 (2009) 642.
7. Li X., Deng S., Fu H., Li T., *Electrochim. Acta*. 54 (2009) 4089.
8. Dafali A., Hammouti B., Kertit S., *J. Electrochem. Soc. Ind*. 50 N°2 (2001) 62.
9. Zouitini A., KandriRodi Y., Elmsellem H., Steli H., Ouazzani Chahdi F., Ouzidan Y., Sebbar N.K., Essassi E.M., El-Hajjaji F., Hammouti B., *Der Pharma Chemica.* 8(10) (2016) 23-31.
10. Benabdellah M., Touzani R., AounitiA., Dafali A., Elkadiri S., Hammouti B., Benkaddour M., *Phys. Chem. News*. 37 (2007) 63.
11. Rallas S., Gulerman N., Erdeniz H., *Farmaco* 57 (2002) 171.
12. Zarrouk A., Zarrok H., Salghi R., Hammouti B., Al-Deyab S.S., Touzani R., Bouachrine M., Warad I., Hadda T.B., *Int. J. Electrochem. Soc.* 7 (2012) 6353-6364.
13. Xiao-Ci Y., Hong Z., Ming-Dao L., Hong-Xuan R., Lu-An Y., *Corros. Sci*. 42 (2000) 645–653.
14. Kandemirli F., Sagdinc S., *Corros. Sci*. 49 (2007) 2118–2130.
15. Ogretir C., Calis S., Bereket G., *J. Mol. Struct. (Theochem)* 635 (2003) 229–237.
16. Bourichi S., Kandri Rodi Y., Elmsellem H., Steli H., Ouzidan Y., Sebbar N.K, Ouazzani Chahdi F., Essassi E.M., El-Hajjaji F.,Hammouti B., *Der Pharma Chemica* 8(10) (2016) 179-186.
17. Wang D., Li S., Ying S., Wang M., Xiao H., Chen Z., *Corros. Sci*. 41 (1999) 1911–1919.
18. Bouoidina A., El-Hajjaji F., Chaouch M., Abdellaoui A., Elmsellem H., Rais Z., Filali Baba M., Lahkimi A., Hammouti B., Taleb M., *Der Pharma Chemica* 8(13) (2016) 149.
19. Ju H., Kai Z.P., Li Y., *Corros. Sci*. 50 (2008) 865–871.
20. Feng Y., Chen S., Zhang H., Li P., Wu L., Guo W., *Appl. Surf. Sci*. 253 (2006) 2812–2819.
21. Sahin M., Gece G., Karcı F., Bilgic S., J. *Appl. Electrochem*. 38 (2008) 809–815.
22. Ozcan M., Dehri I., Erbil M., *Appl. Surf. Sci*. 236 (2004) 155– 164.
23. Salim R., EchChihbi E., Oudda H., ELAoufir Y., El-Hajjaji F., Elaatiaoui A., Oussaid A.,Hammouti B., Elmsellem H., Taleb M., *Der Pharma Chemica*. 2016, 8(13) 200-213.
24. Lebrini M., Lagrenée M., Vezin H., Traisnel M., Bentiss F., *Corros. Sci*. 49 (2007) 2254.
25. Jeyaprabha C., Sathiyanarayanan S., Venkatachari G., *J. Appl. Polym. Sci*. 101 (2006) 2144.
26. Ech-chihbi E., Salim R., Oudda H., Elaatiaoui A., Rais Z., Oussaid A., El Hajjaji F., Hammouti B., Elmsellem H., Taleb M., *Der Pharma Chemica*.2016, 8(13)214-230
27. Veloz M.A., González I., *Electrochim. Acta*. 48 (2002) 135.

28. EL Aoufir Y., Lgaz H., Bourazmi H., Kerroum Y., Ramli Y., Guenbour A., Salghi R., El-Hajjaji F., Hammouti B., Oudda H., *J. Mater. Environ. Sci.* 7 (12) (2016) 4330-4347.

29. Karzazi Y., Belghiti M.E., El-Hajjaji F., Boudra S., Hammouti B., *J. Mater. Environ. Sci.* 7 (11) (2016) 4011-4023.

30. Lebrini M., Bentiss F., Vezin H., Lagrenee M., *Corros. Sci.* 48 (2006) 1279–1291.

31. Hosseini S.M.A., Azimi A., *Mater. Corros.* 59 (2008) 41–45.

32. Oguzie E.E., *Corros. Sci.* 50 (2008) 2993–2998.

33. Popova A., Sokolova E., Raicheva S., Christov M., *Corros. Sci.* 45 (2003) 33–58.

34. El-Hajjaji F., Belkhmima R.A., Zerga B., Sfaira M., Taleb M., Ebn Touhami M., Hammouti B., Al-Deyab S.S., EnoEbenso., *Int. J. Electrochem. Sci.* 9 (2014) 4721 – 4731

35. El Ouasif L., Merimi I., Zarrok H., El ghoul M., Achour R., Guenbour M., Oudda H., El-Hajjaji F., Hammouti B., *J. Mater. Environ. Sci.* 7 (8) (2016) 2718-2730

36. Benabdellah M., Touzani R., Aouniti, A., Dafali A., Elkadiri S., Hammouti B., Benkaddour M., *Phys. Chem. News*, 37 (2007) 63.

37. Rallas S., Gulerman N., Erdeniz H., *Farmaco* 57 (2002) 171.

38. Zarrouk A., Zarrok H., Salghi R., Hammouti B., Al-Deyab S.S., Touzani R., Bouachrine M., Warad I., Hadda T.B., *Int. J. Electrochem. Soc.* 7 (2012) 6353-6364.

39. Ma H., Chen S., Liu Z., Sun Y., J. *Mol. Struct. (THEOCHEM)* 774 (2006) 19.

40. Musa A.Y., Mohamad A.B., Kadhum A.H., Takriff M.S., Ahmoda W., J. *Ind. Eng. Chem.* 18 (2012) 551.

41. Khaled K.F., Al-Qahtani M.M., *Mater. Chem. Phys.* 113 (2009) 150–158.

42. Fu J., Li S., Wang Y.,*J. Mater. Sci.*45 (2010) 6255.

43. Hasanov R., Sadikoglu M., Bilgic S., *Appl. Surf. Sci.* 253 (2007) 3913.

44. Mulliken R.S., *J. Chem. Phys.* 2 (1934) 782.

45. Sanderson R.T., Chemical Bonds and Bond Energy; Academic, New York. 1976.

46. Obot I.B., Gasem Z.M., Umoren S.A.*, Int. J. Electrochem. Sci.*, 9 (2014) 510 – 522.

47. Iczkowski R.P., Margrave J.L., *J. Am. Chem. Soc.* 83 (1961) 3547.

48. Pearson R.G., *Inorg. Chem.* 27 (1988) 734.

49. Yang W., Parr R.G., *Proc. Natl. Acad. Sci.* 82 (1985) 6723.

50. Lgaz H., Salghi R., Larouj M., Elfaydy M., Jodeh S., Rouifi Z., Lakhrissi B., Oudda H., *J. Mater. Environ. Sci.* 7 (12) (2016) 4471-4488.

51. Awad M.K., *Can. J. Chem.*, 91 (2013) 283.

52. Danaee I., Ghasemi O., Rashed G.R., Rashvand Avei M., Maddahy M.H., *J. Mol. Struct.* 1035 (2013) 247–259.

53. Ramya K., Mohan R., Anupama KK., Joseph A.,*Mater Chem Phys.* 149–150 (2015) 632–47.

54. Obot IB., Gasem ZM. *Corros Sci.* 83 (2014) 359–366.

55. Guo L., Ren X, Zhou Y., Xu S., Gong Y., Zhang S., *Arab J Chem.*

56. Kovacevic N., Kokalj A., *J. Phys. Chem. C.* 115 (2011) 24189.

57. Lukovits I., Kalman E., Zucchi F., *Corrosion* 57 (2001) 3.

(2017) ; http://www.jmaterenvironsci.com